IEEE Access
Multidisciplinary | Rapid Review | Open Access Journal

Received 10 January 2024, accepted 20 February 2024, date of publication 26 February 2024, date of current version 7 March 2024.

Digital Object Identifier 10.1109/ACCESS.2024.3369914

RESEARCH ARTICLE

An Evaluation of Battery Degradation and Predictive Methods Under Resistive Load Caused by Intermittent Solar Radiation

KRISHNA KUMBA[1], SISHAJ P. SIMON[2], VENKATESWARLU GUNDU[3], PATRI UPENDER[1], NAWIN RA[1], AND MITHUN SARKAR[1]

[1]Vellore Institute of Technology, Chennai, Tamil Nadu 600127, India
[2]National Institute of Technology Tiruchirappalli, Tiruchirappalli, Tamil Nadu 620015, India
[3]Koneru Lakshmaiah Education Foundation, Vaddeswaram, Guntur, Andhra Pradesh 522302, India

Corresponding author: Krishna Kumba (krishna.kumba@vit.ac.in)

This work was supported by the Vellore Institute of Technology, Chennai, Tamil Nadu, India.

ABSTRACT The most versatile resource for storing energy is one that can rapidly charge or discharge while supporting the use of renewable energy. As renewable energy sources advance rapidly, batteries play a pivotal role in this progress. When integrating battery energy storage into a renewable energy system, it's crucial to address the issue of battery degradation while implementing operational strategies. Furthermore, since solar irradiation varies due to changing cloud conditions, it can impact how batteries charge and discharge. This study focuses on investigating battery degradation and lifetime. Experimental work is being conducted with lead acid batteries connected to a solar photovoltaics system. The paper provides a detailed investigation of commonly used methods for predicting battery lifespan. It also analyzes aspects such as the effects of depth of discharge (DoD) and battery charge/discharge on temperature changes due to degradation. Using the coarse average approach, global battery aging, weighted Ah aging method, and RFC method, this paper estimates the DoD, temperature, life cycle loss (%), and lifespan and evaluates the extent of battery degradation. The battery lifespan is estimated using this method to be 8.42, 8.72, 8.33, and 8.93 years, respectively.

INDEX TERMS Battery lifetime, solar energy, photovoltaic, average approach, global battery aging, rain flow counting method, weighted Ah aging model.

I. INTRODUCTION

In recent years, the integration of renewable energy sources, such as solar power, has become an increasingly pivotal component of sustainable energy systems. As we transition towards cleaner and more efficient energy solutions, understanding the performance and degradation of energy storage systems, particularly batteries, under dynamic conditions becomes paramount. Integrating photovoltaics (PV) with batteries is challenging due to the inherently intermittent nature of solar radiation. However, in the presence of intermittent solar radiation, evaluating the degradation of battery systems is significant. The identification of a battery degradation method reduces battery losses as well as makes the battery healthy. Through a comprehensive analysis, the research sheds light on the nuanced intricacies of battery behavior, fostering advancements in sustainable energy storage technologies.

The PV coupled batteries are optimal sizing for the household's economic viewpoint, and batteries have peak saving potential [1]. A lead-acid battery consists of a chemical storage device that converts chemical energy into electricity. In addition to their design being resistant to temperature, lead-acid batteries are highly reactive to chemical reactions. Battery performance is affected by the environment in which it is used.

Renewable energy sources are currently being subsidized and are receiving financial assistance from the government through various schemes and subsidies. Moreover, in power grid applications the use limit allows up to 100 MW for lead-acid batteries technology and 1MW for lithium technology [2], [3]. Normal lithium batteries are used in static

The associate editor coordinating the review of this manuscript and approving it for publication was Vitor Monteiro.

applications like hybrid vehicles due to their low weight and high performance [4], [5], [6]. However, to increase the battery's lifespan the manufacturers recommended that maintain battery temperature be 25°C to 35°C [7]. To temperature rising of batteries are significant battery capacity and power degradation. The result is higher degradation due to charge and discharge increase cell temperature. Therefore, this is considered as one of the reasons for the degradation rate of the battery. Every 10°C temperature increase would be double the battery degradation, experimentally analysis carried out [8].

The temperature and various cycles of charging and discharging can cause loss in a lead-acid battery. Temperature increases could the number of life cycles decreases. The manufacturer evaluated the temperature effect of the battery, the life decreases when the temperature has increased in the range of 20°C to 50°C. According to Arrhenius' law each rise of temperature 10°C above 20°C, the GEL SOLAR VRLA battery lifetime reduces the rate by 50%. All lead-acid batteries are not affected by the percentage reduction. On comparing GEL VRLA batteries with GEL VRLA lead-acid SOLAR batteries, the temperature influence is less than 20%. Here, flooded lead-acid type batteries are used in this work for inquiry purposes [9], [10].

In order to explore the aging model, Rodolfo et al. evaluated the lifespan of lead-acid batteries combined with an autonomous the PV. Here, the charge controller is investigated [11]. Lead-acid batteries with PV system mathematical models were proposed by Copetti et al. to track temperature variations caused by changes in internal resistance and battery capacitance [12]. Lead-acid technology longevity coupled to a hybrid wind and solar PV system has been studied by Schiffer et al. [13]. A model predictive control technique was put up by Cai et al. for structures with on-site solar energy production and battery generation. This model was created offline using degradation data and a capacity loss model with a physical foundation [14]. Collath et al. [15] utilized aging aware process to increase the lifetime productivity of battery energy storage system (BESS). In this case, the importance of model predictive control (MPC) over the current method of choosing ageing cost based on BESS cost has been highlighted in terms of enhancing the lifetime predictability of a BESS. The latest developments regarding the grid-connected PV battery systems' operation approach were examined by Zhang et al. [16]. The study has revealed that the multi objective parameter study on a large-scale system is the need of the hour. The ageing and performance degradation of the system over time must be taken into account when studying large-scale BESS systems [17]. The challenges in aging prognostics have been discussed by Liu et al. [18]. The application of transfer learning technology for battery management has been proposed in the work. But the existing studies have not discussed the practical validation of the results. The results of the aging prediction study are crucial for optimal operation and maintenance of the system.

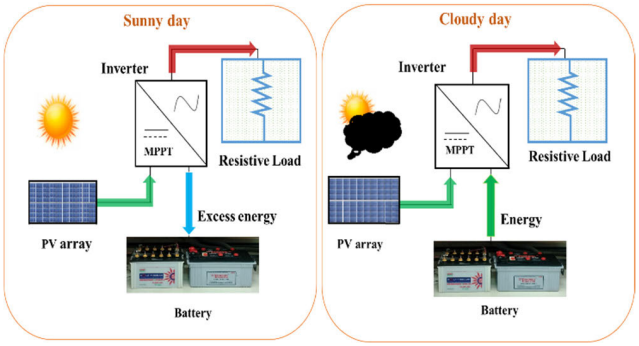

FIGURE 1. Schematic diagram of system model.

The existing research findings have not investigated the issues in intermittent solar radiation of PV with BESS, and the comparison among different methods has not been done in detail. The solar irradiation varies based on weather conditions, which can impact the charge and discharge operation of batteries when batteries are integrated between PV and load. As a result, the charge and discharge of the battery DoD is affected, and the temperature is raised. Batteries lose their useful life due to improper DoD and temperature effects. Therefore, the main objective of the work is as follows,

i. To estimate the lifespan of a lead-acid battery that is integrated with photovoltaic technology.

ii. To estimate the parameters such as ageing rate (%), loss (%), and lifetime (Years) using Global battery aging model and Rain-flow counting methods.

iii. The life cycles of battery are estimated using the Coarse average approach and Weighted Ah methods.

iv. An explanatory analysis is provided to show how intermittent solar radiation of PV with battery and temperature varies to battery degradation concerning charging and discharging current.

Realistic results are produced because the explanation scenarios are based on genuine BESS operation. Figure 1 shows the model's work schematic diagram for the PV combined with a battery system. In this work for the investigation purpose, flooded lead-acid type of batteries is used.

The rest of the article is organized as follows: In section II, solar PV system, battery selection, and lifetime factors influence of battery have been detailed. The battery life prediction approaches have been discussed Section III. In Section IV the established system and results have been discussed and analyzed. The discussion of battery lifetime estimation methodologies concludes in Section V.

II. PHOTOVOLTAIC AND SELECTION OF BATTERIES AND FACTORS THAT INFLUENCE BATTERY LIFE

A. PHOTOVOLTAIC SYSTEM

The installation sites are highly affected by solar irradiance and ambient temperature profiles, which affect the PV generation output. The net solar radiation (G_{net})W/m^2 falling on

the PV module surface can be obtained from equation (1). Here, $G_{dir\ coll}$, $G_{diff\ coll}$ are the direct, diffuse solar radiation on the PV module. G_{ground_ref} is ground reflected solar radiation from the ground surface. $G_{right\ ref}$ and $G_{left\ ref}$ are right and left side reflected solar radiation on the PV module surface.

$$G_{net} = G_{dir\ coll} + G_{diff\ coll} + G_{ground\ ref} + G_{right\ ref} + G_{left\ ref} \quad (1)$$

Solar radiation is absorbed directly from the sun without being dissipated by the atmosphere. The direct solar radiation ($G_{dir\ coll}$) can be obtained from equation (2).

$$G_{dir\ coll} = G_{in} \sin(\alpha + \beta) \quad (2)$$

By using equation (3), you can estimate the annual PV energy (ΥEO) output in kWh.

$$\Upsilon EO = G^{*}_{IPR} A_{PV} \eta_{PV} PR \quad (3)$$

Here G^{*}_{IPR}, A_{PV}, η_{PV}, and PR represents the solar radiation (kWh/m^2/yr), PV system area (m^2), PV panel efficiency (η_{PV}), and performance ratio (PR), respectively [19].

B. SELECTION OF BATTERIES

Six considerations are taken into account while selecting a battery type. The first factor to take into account is design capacity time, or how long the battery can run the system before needing to be charged once again. The second factor is battery ageing, or the decline in battery performance brought on by ageing. Lead-acid batteries' behavior is regulated by five factors. The temperature adjustment, specified in the IEEE Standard 485, is the third factor. The capacity rating, which controls voltage depression and determines the battery's charge holding capacity when fully charged, is the fourth factor. The fifth factor is the nominal battery voltage or the voltage of a completely charged battery without any load. The battery's maximum depth of charge, or how much it can be depleted before it needs to be recharged, is the sixth consideration. Equation (4) can be used to calculate the minimum battery capacity (C_i) when all these components are taken into account, which aids in choosing the right battery size.

$$C_i = \frac{E_d(k_a * k_t * k_c)}{V_{dc} * DoD_k} \quad (4)$$

where E_d is the energy over autonomy time in Ah. k_a, k_t, and k_c are the battery ageing, capacity rating, and temperature correction factors in %. V_{dc} and DoD_k are the battery voltage and DoD cycle.

The overall charging time is one factor to take into account when charging the battery. Equations (5) and (6) below illustrate the process used to determine the lead-acid battery's charging time (t). 52 Ah is found to be the size of the used battery. A typical charger has a constant of 1.4. Therefore, 72.8 Ah of energy is required to charge the battery. The energy required will be divided by 17.50 A, the initial charge current, as the charger will be of the standard kind. The suggested system needs 4.16 hours to fully charge. Although both chargers are of the standard sort, charging from a PV panel will take more time than charging from an AC supply.

$$E = 1.4 * C_i \quad (5)$$

$$t = \frac{E}{17.50} \quad (6)$$

where, E and C_i are the energy needs to charge and initial battery capacity in Ah.

A solar panel's output is measured in watts. When the solar panel is exposed to direct sunlight, it will produce around 1 Ah for every 15 watts that it is rated for. At 25°C, the solar panel was rated for 87 W, which translates to 5.8 Ah per hour. The PV panel will produce a DC voltage between 13 and 17 volts as its output. The voltage was increased via a power boost converter to 48V. The DC-DC converter performs better than other devices in terms of peak output power and output voltage. A safety mechanism on the solar charge controller prevents the battery from being overcharged. Moreover, this controller will be able to detect when the battery's voltage is dropping. To ensure the battery's safety, the controller will off the power at this moment.

In order to obtain accurate readings, the battery must rest in an open circuit for at least four hours; lead-acid batteries should rest for 24 hours. Thus, for an active battery, the voltage-based status of charge (SoC) method is not feasible (7). The DoD of the battery is expressed as a percentage of its initial capacity. The SoC and DoD are viewed as complements to one another. Equation (8) can be utilized to compute the DoD. Here, the battery discharge current ($I_{discharge}$) in the interval of initial time (t_i) to final time (t_f).

$$SoC = 100 - DoD \quad (7)$$

$$DoD = \frac{\int_{t_i}^{t_f} I_{discharge} dt}{C_i} \quad (8)$$

C. BATTERY LIFETIME INFLUENCE FACTORS

1) DEPTH OF DISCHARGE (DOD)

Solar lead grid-plate batteries are a type of starter batteries that have been modified for use in solar applications. These batteries have thicker plates with a larger spacing and are made with hardened lead that contains antimony. They have a meagre lifespan of just 4000 cycles if they are discharged to a maximum of 20% of their capacity, which is known as a DoD of 80%. Figure 2 shows that these batteries can reach 3500 cycles for a discharge of only 20%. As a result, solar lead grid-plate batteries are suitable for sporadic use, such as in weekend cottages.

2) TEMPERATURE

The active materials of the battery undergo corrosion reactions under dynamic operating conditions. The phenomenon of this results in battery resistance increases due to this the battery capacity is decreased. Hotter conditions, the chemical response of the battery is faster. When the battery temperature

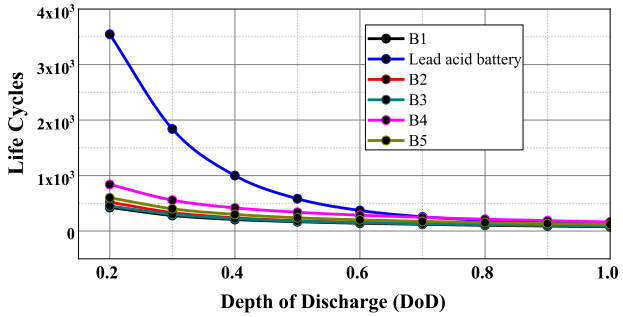

FIGURE 2. Best fit curve to manufacturer's life cycles of different batteries Vs. DoD.

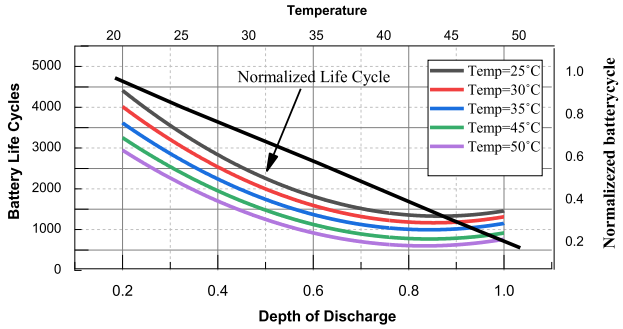

FIGURE 3. Battery life cycles degradation at different temperatures and normalized life cycle with temperature for a lead-acid battery.

is high, unwanted reactions also occur. Figure 3 depicts the battery life cycle degradation at different temperatures and normalized life cycles with temperature for a lead-acid battery. In figure clearly indicates that 20% of DoD normalized life cycles are more. In addition, observe that, when the battery temperature is changing the battery life cycle curve also changes as a parabolic shape.

In order to determine the temperature versus the number of life cycles (N), the following points must be considered. Battery operating temperature is in °C. The percentage of battery cycles (Nc(%)) can be calculated using equation (9). The life cycles variation of the battery with temperature the mathematical model is given in equation (10). T [°C] = [20 25 0 40 50], Nc [%] = [100 75 50 25 12.5]. The operating temperature of battery equals ambient temperature (Ta) and changed temperature (ΔT) of the battery, which is T=Ta+ΔT. Here, $N_{C(DoD)T}$ is at the temperature (T) maximum life cycles [20].

$$\mathrm{Nc}(\%) = \frac{\mathrm{N_{C(DoD)T}}}{\mathrm{N_{C(DoD)20°}}} \tag{9}$$

$$N_{C(T)\%} = \begin{cases} 100 & 0 < T \leq 20°C \\ 3.68\mathrm{T}^{-1.101} - 0.3897 & T > 20°C \end{cases} \tag{10}$$

III. BATTERY LIFE PREDICTION APPROACHES

The battery is a combination of electrochemical systems that requires a detailed appreciation of the aging model and its causes. The lifetime estimation methods must provide reliable results to be valuable. The lifetime assessments are estimating the result of changes in operating conditions of battery characteristics. Therefore, briefly discussed life prediction approaches.

A. PHYSIC AND CHEMICAL AGEING APPROACH

The battery performance has gradually increased in the operating and cycles-defined deterioration index. When the battery hits the threshold value, its life is over and it must have been terminated. The internal chemical reaction and several stress factors, such as operating temperature, battery charge and discharge, and DoD, all contribute to the battery degradation rate. The SoC, DoD, and temperature could be used to evaluate battery life. A proposed crack theory quantifies the stress factors [15]. Millner. A explained the detailed aging at 15°C and 35°C four kinds of different charge-discharge methods [16], [17], [18], [20].

B. COARSE AVERAGE APPROACH

The average DoD and average battery operating temperature serve as the primary inputs for determining battery lifetime. This is a simple approach for estimating battery lifetime that is based on energy throughput and overall DoD. This method is the least computationally intensive approach of the two because, as given in equations (11) and (12). All the data points collected during the simulation are averaged to calculate DoD and temperature.

$$\overline{DoD} = \frac{\sum_{i=1}^{N} DoD_i}{N} \tag{11}$$

$$\overline{T} = \frac{\sum_{i=1}^{N} T_i}{N} \tag{12}$$

where *overlineDoD*, T, and N are the average DoD, average temperature, and data points used in the simulation. As a result, the battery lifespan is determined using equation (13).

$$\mathrm{L_{time}} = n * \bar{DoD} * \frac{2 * E_{BatCap}}{E_{BatEne}} \tag{13}$$

where $\mathrm{L_{time}}$ = Lifetime of battery in years, n = Cycle-life, $\bar{DoD}$ = Average active DoD, E_{BatCap} = Capacity nominal of the battery, E_{BatEne} = Energy output overall from the battery [21].

C. GLOBAL BATTERY AGING MODEL

The maximum cycle count ($N_{C(DoD)T}$) for each DoD and temperature has been calculated as follows:

$$N_{C(DoD)T} = \begin{cases} \left(12,850e^{-(9.738*DoD)} + 3210e^{-(1.429*DoD)}\right) \\ 0 < \mathrm{T} \leq 20°\mathrm{C} \\ \left(12,850e^{-(9.738*DoD)} + 3210e^{-(1.429*DoD)}\right) \\ * \left(3.68\mathrm{T}^{-1.101} - 0.3897\right) \\ \mathrm{T} > 20°\mathrm{C} \end{cases} \tag{14}$$

A minimal effect of temperature on battery ageing (R_a) is expected in the range 0-20 °C. By taking the inverse of the number of cycles determined (k), the ageing rate is determined for each cycle. The following equation provides the expression:

$$R_{a/C(DoD_k)T_k} = \frac{1}{N_{(DoD_k)T_k}} \tag{15}$$

where k is depicting the cycle's index out of all the cycles. The equation in (16) explains how to determine the ageing rate R_a for N_C cycles. When the cumulated rate approaches the unit's, battery is near the end of its useful life [21], [22], [23], [24].

$$R_a = \sum_{k=1}^{N_C} R_{a/C(DoD_k)T_k} \tag{16}$$

D. WEIGHTED AH AGEING APPROACH

The National Renewable Energy Laboratory (NREL) states that at rated power and rated DoD, the battery can give stable energy. It's called the total real discharge of the battery [25]. If the total real discharge is equal to cumulative effective discharge, then life is ending, and it needs to terminate. Different DoD and discharge rates of lead-acid battery operating characteristics are experientially confirmed by NREL. Energy storage capacity optimization and dispatch strategy are auxiliary tools of this model [26]. The weighted Ah method shows the effect of DoD on battery life in equation (17).

The weighted Ah aging method creates the basic assumption. Because the same quantity at different SoC levels affects the battery life loss, this method is irrelevant to DoD. It takes into account the various ways that DoD, temperature, charge, and discharge might affect a battery's lifetime. Hence, it defaults to add the weighted coefficient to this method. This method can be used with the assumption that the battery will reach Ah throughout its life, even under these test conditions. The battery must be changed when the effective value is more than the threshold value. The equation (17) is rearranged for the getting parameters of equation (18) [27], [28], [29].

$$L_A = L_R \left(\frac{D_A}{D_R}\right)^{u_0} e^{u_1\left(1-\left(\frac{D_A}{D_R}\right)\right)} \tag{17}$$

$$\frac{\mathrm{d_{eff}(D_A)}}{\mathrm{D_R C_R}} = \frac{\mathrm{L_R}}{\mathrm{L_A}} \tag{18}$$

$$2L_A.d_{eff}\ (D_A)\ i = 2L_A D_R C_R \left(\frac{\mathrm{L_R}}{\mathrm{L_A}}\right) = 2L_A D_R C_R \tag{19}$$

where, D_A, D_R, L_A, *and* L_R are actual DoD, rated discharge, DoD on cell life, and arbitrary DoD (D_R) number of battery life cycles. $2\mathrm{L_R D_R C_R}$ is the battery's total effective amount, which is a fixed value. $\mathrm{d_{eff}(D_A)}$ discharge is adjusted by depth and rate in AH, $C_R$is AH capacity of battery cell, u_0, and u_1 are the battery linear curve fit. In order to evaluate battery performance, power density and energy density are the most important metrics. The battery Ragone curve can be used to calculate the battery capacity [30], [31]. The battery size, denoted as $\mathrm{d_{eff}}$, is at the appropriate charge and discharge power. d_{actual} is a representation of the battery quantity at actual charge and discharge. As the rate increases, the true quantity will increase according to the Ragone curve. Equation (20) outlines the relationship.

$$\frac{d_{eff}}{d_{actual}} = \frac{C_R}{C_i} \tag{20}$$

The total Ah capacity of a cell (C_i) is not fixed and depends on the DoD at which it is cycled. This means that the actual Ah discharged in each cycle may be less or more than the rated capacity, depending on the rated DoD relative to the actual DoD. Equation (21) can be used to calculate the battery's lifetime.

$$\mathrm{L_{time}} = \left(\frac{2\mathrm{L_R D_R C_R}}{\sum \mathrm{d_{eff}}}\right) \mathrm{T} \tag{21}$$

E. AGEING APPROACH OF EVENT-ORIENTED METHOD

Many different counting techniques exist, such as cross-level counting, peak counting, simple range counting, and rain flow counting (RFC). The RFC algorithm is different from other counting methods. It was created previously to turn a range of complex stress problems into a set of straightforward stress problems for the analysis of fatigue data. In the context of lifetime estimation, the rain flow algorithm itself is interesting as a method to decrease a spectrum of changing temperatures to a set of simple temperature reversals. The practical definition of the RFC is explained in American Society for Testing and Materials (ASTM) E-1049-85. Standards are developed and disseminated by ASTM, a global organization for standards [32].

By referring to the whole (or) SN curve in many areas of engineering, predicting the lifetime in the standard approach manner can get the best results. Whole (or) SN curve S(t) is generally used for design and assessing a lifetime of components. These methods easily apply to the electrochemical systems for the prediction of a lifetime if the system's conditions are fulfilled. Moreover, this method is most suitable for a fast assessment of system design and working plans. In addition, this method can also easily be used for operating plans in online changes. Figure 4 shows the terminology used for irregular loading histories, and the most important concept is explained below.

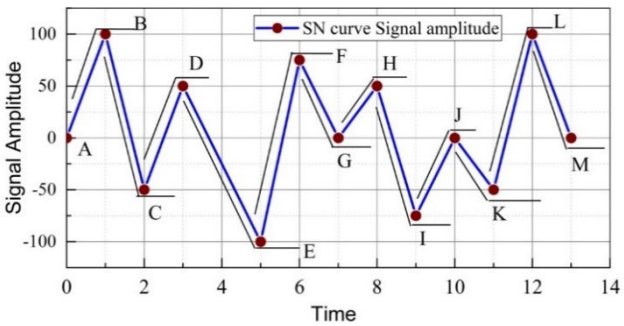

FIGURE 4. SN cycle extraction using the RFC.

Here are some clarifications regarding rain flow path analysis:

i A rain flow path, starting at point A (the origin), will follow the ''pagoda roofs'' until it reaches a valley with a lower value than the origin. In the given figure, the path starting at A ends at point C.
ii A rain flow path is concluded when it intersects with a previously analyzed path. For instance, the path starting at C is terminated in the diagram.
iii New paths are not initiated until the current path has ended.
iv For the full data set, valley-generated half-cycles are specified. The mean SN is the midpoint, and the stress range SN is the vertical distance covered by a path for each cycle.
v For peak-generated rain flow routes, the same method is applied in reverse by coinciding each valley-generated half-cycle with a peak-generated half-cycle to form a complete cycle.

Applying the above-discussed Rain flow algorithm methodology for battery charge and discharge curve, because of the SoC signal has given an interesting result. Comparative system aging for relative degradation of each cycle represents. In the process, the DoD cycle represents DoD_k, of two successive half cycles of mean depth. The conversion coefficient can be calculated using equation (22).

$$\alpha\,(x) = \frac{N_{BESS}(1)}{N_{BESS}(k)} \tag{22}$$

where $\alpha(k)$ [6] is a conversion coefficient. $N_{BESS}(k)$ are several battery cycles at the constant depth of discharge k(DoD), this is obtaining on the SN curve. The equation (23) defines the battery charge and discharge cycles during the investigation interval.

$$N^{i}_{BESS} = \sum\nolimits_{1}^{n} \alpha\,(k_i) \tag{23}$$

The depth of discharge of every charge and discharge cycles as a limit $k_i(1 \leq i \leq n)$, where n is total no of charge and discharge cycle. When $N^{i}_{BESS} = N_{BESS}$, it indicates that the battery life is ended [33]. Equation (24) and (25), can estimate the loss of life cycles during the time of the investigation. it is the total losses of the cycle's degradation.

$$Loss_i = \frac{1}{N_{BESS}(k_i)} \tag{24}$$

$$Loss = \sum\nolimits_{1}^{n} Loss_i = \sum\nolimits_{1}^{n} \frac{1}{N_{BESS}\,(k_i)} \tag{25}$$

IV. A CASE STUDY OF AN ESTABLISHED BATTERY INTEGRATED WITH PV SYSTEM

After defining the methodologies for the battery lifetime calculation, the case study of an established battery integrated with a PV system and a resistive load (1.5 kW) is presented in Figure 5. During the evaluation of the battery, capacity power ratings, depth of discharge (DoD), temperature, efficiency, warranty, and manufacturer should be considered. Temperature and DoD have significantly impact on solar batteries, hence, protecting them from freezing temperatures or scorching heat, and over-current charge/discharge can extend their useful lives. PV batteries will require more voltage when the temperature drops below 30° F (−1.11° C); when the temperature rises above 90° F (32° C), they will become overheated and require a reduction in voltage.

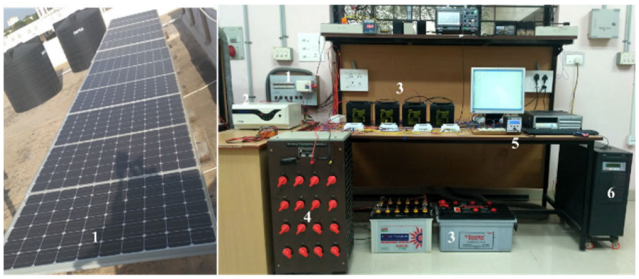

1. PV Array, 2. MPPT Charge Controller, 3. Batters, 4. DC load, 5. Data Logger, 6. Grid connected Inverter

FIGURE 5. Practical experimental setup.

Moreover, the most important point while connecting the battery with the PV system: the PV is dependent on solar radiation and temperature, which are unpredictable and change with the weather. Therefore, a charge controller in this model guards against overloading the batteries. By implementing a specific deep-discharge prevention system that disconnects the load if the voltage drops too low, the battery is shielded from damage. The established system specifications of PV array, and battery are shown in Table 1 and 2. Here, a dynamic simulator is developed for the established system shown in Figure 6. The simulator has considering significant parameters like battery discharge current the battery temperature, DoD due to electrical load, and the ambient temperature, etc.,

TABLE 1. 1.5 kW PV array panel specification.

Description	Value
Peak power	100 W
Number of cells	36
Open circuit voltage	21.06 V
Maximum voltage	24.3 V
Short circuit current	5.16 A
Maximum current	7.61 A
Series resistance	0.21 Ω
Parallel resistance	402.1 Ω
Temperature coefficient of sc	0.00321 A/K
Temperature coefficient of oc	-0.124 V/K

According to the theoretical design and evaluation, the battery subsystem is comprised of four lead-acid batteries that are connected in both parallel and series. The system will run

TABLE 2. Constraints used for battery model.

Description	Value
Battery voltage constant	24 V
Battery capacity	26 Ah
Fitting parameter	0.24
Internal resistance	0.318 Ω
Energy over autonomy time	1200 VAh
Aging factor	25 %
Temperature factor	1
Capacity evaluation	4.5 %
DoD	20%

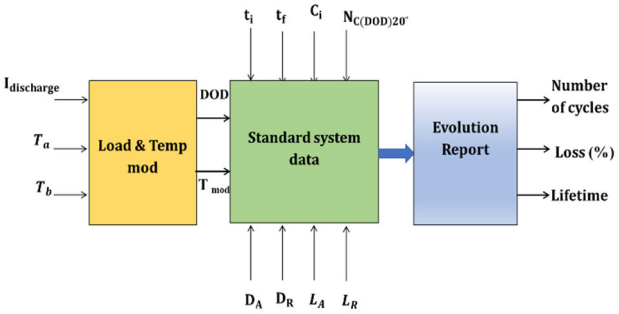

FIGURE 6. Dynamic simulator.

on a total voltage of 48V, which is obtained by connecting two 24 V lead-acid batteries in series. The selection of this battery is primarily based on its runtime expressed in ampere-hours (Ah), which is crucial for ensuring that the system runs for a sufficient period. Besides, this battery has a high ability to retain a charge for almost three months, with just a 9% capacity loss, making it an excellent choice for the application. Battery Energy Storage System (BESS) performs only according to the scheduled of charge and discharge condition, whereas, the output availability of the PV.

Before going to investigate the battery degradation due to the intermittent solar radiation effects of PV integrated with a batter system, the control strategy of BESS used in the work is described briefly below.

The BESS main three power control strategies are followed. (i) When there is more availability of output PV power, batters are charged according to predefined control charging strategies. (ii) In cases where solar PV output is affected by passing clouds, the BESS power is used as a substantial source to limit improper ramp rates of the PV plant. (iii) A battery can be used as a source of power in the event of PV power being unavailable. Here, assuming a 20-year lifespan for the PV plant, battery-rated life cycles are limited to 3500 at 20% depth of discharge per day, as shown in Figure 2. To maintain these limitations, the SoC of BESS is kept within the 50% to 90% range. The manufacturer has specified a maximum depth of discharge limit of 50%, which allows the highly variable output of the PV plant to still be useful. It is implemented in coupling topologies in the same way, and inverter efficiency depends on output power and connection topology.

The data is taken every five minutes from the 1.5 kW PV array and the BESS system to determine the accuracy of our analysis from Jan-22 to Jun-22. Here, three different days are using to analyzing how can be the PV output effect battery life cycles. The output of the 1.5 kW PV array of three different days is shown in Figure 7. The battery PV energy and battery energy sharing profile is presented in Figure 8. The figure shows that on the clear day-1 fully radiation day there is no variability of output of the PV system. Day 2 is a slight variation of the output of the PV array. Here, day 3 is more variated compared to day 1 and day 2 due to the variability of solar radiation changes. Same and constant load profile is used for all days.

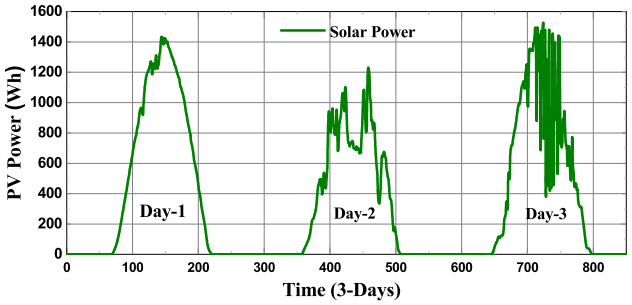

FIGURE 7. Three different days PV power profile.

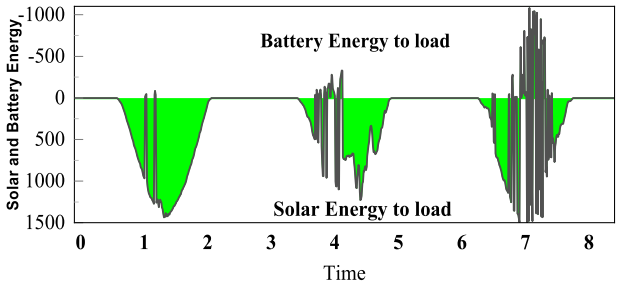

FIGURE 8. Solar energy and battery energy sharing profile.

In Figure 9(a), the battery energy cycles and solar energy are displayed. The battery cycles indicate when the battery energy is delivered to the load due to the unavailability of PV output. Figure 9(b) shows the histogram variation, particularly on day two and day three, in the range of 100. To charge the battery completely to its rated capacity of 1.24 kWh, approximately 1.4 kWh/m^2 of solar radiation is required.

Figures 10(a) and 10(b) show three different days of the battery temperature and ageing rate. In this figure clearly shows that day-2 and day-3 variations of battery temperature. Here, day-2 is a slight variation, and day-3 high variation of battery temperature. Figures 10(a) and 10(b) show battery aging rates calculated using the procedure explained in section II of the paper. The battery temperature changes

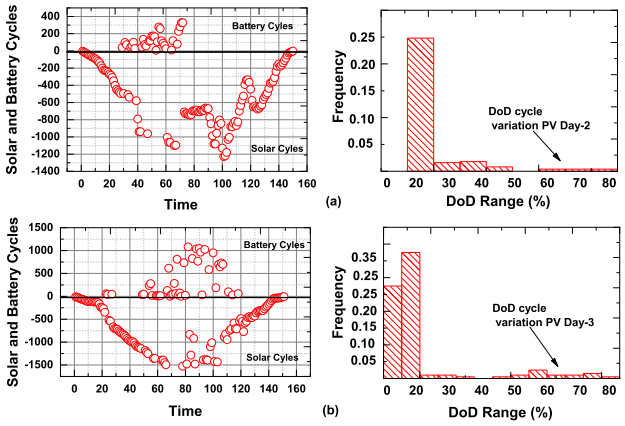

FIGURE 9. Battery energy provided to the load calculated using five-minute data, data histograms in (a) slightly variable PV day-2 and (b) extremely variable PV day-3.

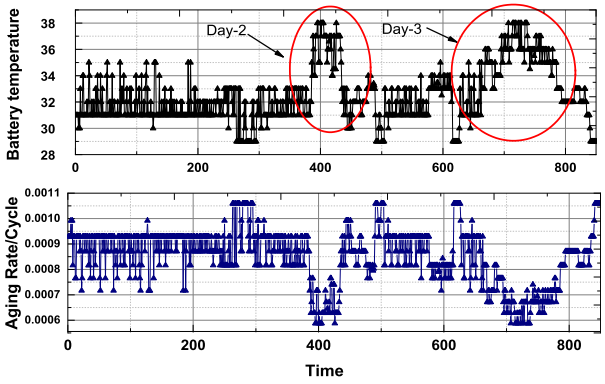

FIGURE 10. 10 (a) Battery temperature profile and 10 (b) Evolution of aging rate $N_{C(DOD)T}$ as a function of k cycle.

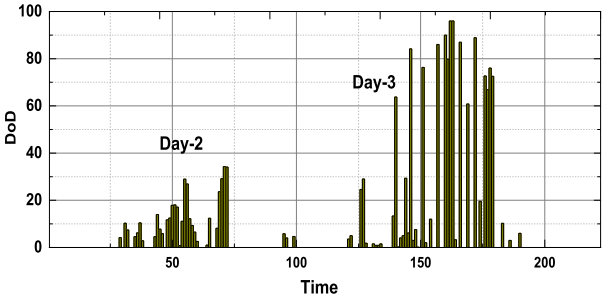

FIGURE 11. Battery DoD profile.

due to battery DoD, because of the variability of PV output. We can observe in Figures 10(b) the aging rate also changes concerning battery temperature.

The histogram profile of partial cloudy (Day 2) and cloudy (Day 3) of BESS due to the intermittent solar radiation is shown in Figure 11. This graph shows that the BESS profile is more influenced on day 3 than on day 2. Table 3 (Day 2 and Day 3) and Table 4 (Jan-22 to Jun-22) shows the aging rate, loss (%), number of battery cycles, and lifetime of the battery based on the above-discussed method methods.

TABLE 3. Battery lifetime estimate based on models.

Methods	Estimated parameters	Day-2	Day-3
Coarse average approach	Number of cycles	21.46	28.45
	Lifetime (Years)	8.17	7.93
Global battery aging model	Number of cycles	16.46	27.82
	Ageing rate (%)	3.99	4.12
	Lifetime (Years)	8.48	8.26
Weighted Ah ageing	Number of cycles	24.46	29.32
	Lifetime (Years)	8.09	7.76
Rain-flow counting	Number of cycles	14.32	24.32
	Loss (%)	3.29	3.49
	Lifetime (Years)	8.66	8.37

The average generated energy of PV and average battery DoD profile from Jan-22 to Jun-22 are shown in Figures 12 and 13. PV system energy generated and battery discharge rate are approximately 5.13 kW and 38%, respectively, on an average daily basis. For the same battery technology, the coarse average approach estimates the battery lifetime is 8.42 years. The global battery aging model estimates the ageing rate and lifetime of the battery are 3.78%, and 8.72 years. Weighted Ah aging method estimates the battery lifetime is 8.33 years. Finally, RFC method estimates the loss and lifetime of the battery are 3.56% and 8.93 years, respectively.

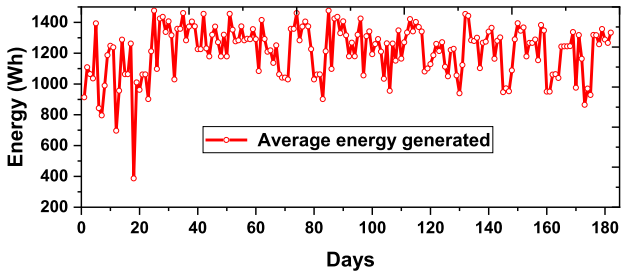

FIGURE 12. Generated energy (Jan-22 to Jun-22).

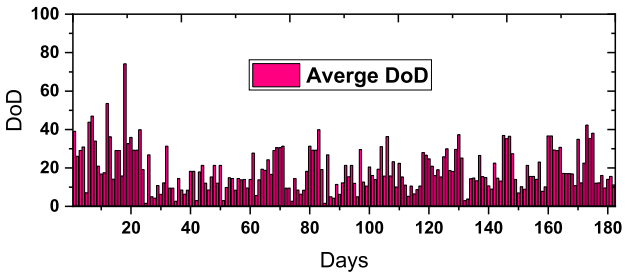

FIGURE 13. Generated energy (Jan-22 to Jun-22).

Each method is located relatively close to each other. However, the perfect estimation of battery lifetime is very critical using mathematical models, physics-based models, RFC, and even machine learning, because the parameters considered are different for each method. Despite these efforts, no accurate predictions were produced since there

TABLE 4. Battery lifetime estimate based on models.

Methods	Estimated parameters	Jan-22 to Jun-22
Coarse average approach	Number of cycles	415
	Lifetime (Years)	8.42
Global battery aging model	Number of cycles	401
	Ageing rate (%)	3.78
	Lifetime (Years)	8.72
Weighted Ah ageing	Number of cycles	420
	Lifetime (Years)	8.33
Rain-flow counting	Number of cycles	390
	Loss (%)	3.56
	Lifetime (Years)	8.93

was a lack of information or the batteries differed chemically. Based on the comparison with different models, it is shown that the simple battery lifetime model described in this paper is capable of estimating battery lifetimes reasonably.

The investigation focused on lead-acid batteries only. Therefore, it can investigate different types of batteries as well as different load conditions in the future. Furthermore, the battery lifetime is estimated using machine-learning models. This research seeks to create a machine-learning model that takes known chemistry as its input dataset and produces an output predicting the life of a battery with unknown chemistry.

V. CONCLUSION

Battery lifetime estimation caused by solar radiation is a critical concern that needs to be addressed in PV systems. The battery degradation and continuous operation are almost significantly difficult to analyze correctly. In order to ensure accurate and reliable results, it is essential to choose the appropriate evaluation method. Therefore, the coarse average approach, global battery aging, weighted Ah aging method, and RFC methods are discussed for this purpose. These four prediction methods work according to different theoretical principles. So here, the effects of life damage factors of the batter are discussed. Battery life prediction approaches and hypothesis mathematical theory models are explained. Moreover, using the global battery aging model and the RFC method estimated the aging rate, loss, number of cycles, and lifetime of the battery. The weighted Ah approach is the most accurate of the four approaches.

REFERENCES

[1] W. L. Schram, I. Lampropoulos, and W. G. J. H. M. van Sark, "Photovoltaic systems coupled with batteries that are optimally sized for household self-consumption: Assessment of peak shaving potential," *Appl. Energy*, vol. 223, pp. 69–81, Aug. 2018.

[2] Z. Shi, W. Wang, Y. Huang, P. Li, and L. Dong, "Simultaneous optimization of renewable energy and energy storage capacity with the hierarchical control," *CSEE J. Power Energy Syst.*, vol. 8, no. 1, pp. 95–104, Jan. 2022, doi: 10.17775/CSEEJPES.2019.01470.

[3] B. B. McKeon, J. Furukawa, and S. Fenstermacher, "Advanced lead–acid batteries and the development of grid-scale energy storage systems," *Proc. IEEE*, vol. 102, no. 6, pp. 953–963, Jun. 2014.

[4] N. Omar, M. A. Monem, Y. Firouz, J. Salminen, J. Smekens, O. Hegazy, H. Gaulous, G. Mulder, P. Van den Bossche, T. Coosemans, and J. Van Mierlo, "Lithium iron phosphate based battery—Assessment of the aging parameters and development of cycle life model," *Appl. Energy*, vol. 113, pp. 1575–1585, Jan. 2014.

[5] D. Simatupang, A. Benshatti, and S.-Y. Park, "Battery internal temperature measurement using LC resonant tank for battery management systems," *Batteries*, vol. 9, no. 2, p. 104, Feb. 2023, doi: 10.3390/batteries9020104.

[6] D. Simatupang and S.-Y. Park, "Integration of battery impedance spectroscopy with reduced number of components into battery management systems," *IEEE Access*, vol. 10, pp. 114262–114271, 2022.

[7] E. Karden, S. Ploumen, B. Fricke, T. Miller, and K. Snyder, "Energy storage devices for future hybrid electric vehicles," *J. Power Sources*, vol. 168, no. 1, pp. 2–11, May 2007.

[8] O. Gross and S. Clark, "Optimizing electric vehicle battery life through battery thermal management," *SAE Int. J. Engines*, vol. 4, no. 1, pp. 1928–1943, Apr. 2011.

[9] S. Gielinger, T. Hein, A. Ziegler, D. Oeser, S. Breitfelder, and G. Bohn, "A short time expansion measurement method for the detection of aging effect of lithium ion cells using a high resolution laser interfometric setup," *IEEE Access*, vol. 11, pp. 139924–139934, 2023, doi: 10.1109/ACCESS.2023.3341505.

[10] *Handbook for Gel-VRLA-Batteries—Part 2, Installation, Commissioning and Operation, Exide Technologies*, document Revision 5, Sonnenschein, Chicago, IL, USA, 2003.

[11] R. Dufo-López, J. M. Lujano-Rojas, and J. L. Bernal-Agustín, "Comparison of different lead–acid battery lifetime prediction models for use in simulation of stand-alone photovoltaic systems," *Appl. Energy*, vol. 115, pp. 242–253, Feb. 2014.

[12] J. B. Copetti and F. Chenlo, "Lead/acid batteries for photovoltaic applications. Test results and modeling," *J. Power Sources*, vol. 47, nos. 1–2, pp. 109–118, Jan. 1994.

[13] J. Schiffer, D. U. Sauer, H. Bindner, T. Cronin, P. Lundsager, and R. Kaiser, "Model prediction for ranking lead-acid batteries according to expected lifetime in renewable energy systems and autonomous power-supply systems," *J. Power Sources*, vol. 168, no. 1, pp. 66–78, May 2007.

[14] J. Cai, H. Zhang, and X. Jin, "Aging-aware predictive control of PV-battery assets in buildings," *Appl. Energy*, vol. 236, pp. 478–488, Feb. 2019.

[15] N. Collath, M. Cornejo, V. Engwerth, H. Hesse, and A. Jossen, "Increasing the lifetime profitability of battery energy storage systems through aging aware operation," *Appl. Energy*, vol. 348, Oct. 2023, Art. no. 121531.

[16] Y. Zhang, T. Ma, and H. Yang, "A review on capacity sizing and operation strategy of grid-connected photovoltaic battery systems," *Energy Built Environ.*, vol. 5, no. 4, pp. 500–516, Aug. 2024.

[17] M. Pakjoo, L. Piegari, G. Rancilio, S. Colnago, J. E. Mengou, F. Bresciani, G. Gorni, S. Mandelli, and M. Merlo, "A review on testing of electrochemical cells for aging models in BESS," *Energies*, vol. 16, no. 19, p. 6887, Sep. 2023, doi: 10.3390/en16196887.

[18] K. Liu, Q. Peng, Y. Che, Y. Zheng, K. Li, R. Teodorescu, D. Widanage, and A. Barai, "Transfer learning for battery smarter state estimation and ageing prognostics: Recent progress, challenges, and prospects," *Adv. Appl. Energy*, vol. 9, Feb. 2023, Art. no. 100117.

[19] N. Pearsal, *The Performance of Photovoltaic (PV) Systems Modelling, Measurement and Assessment* (Woodhead Publishing Series in Energy), 1st ed. U.K.: Joe Hayton, Oct. 2016.

[20] T. M. Layadi, G. Champenois, M. Mostefai, and D. Abbes, "Lifetime estimation tool of lead–acid batteries for hybrid power sources design," *Simul. Model. Pract. Theory*, vol. 54, pp. 36–48, May 2015, doi: 10.1016/j.simpat.2015.03.001.

[21] N. Narayan, T. Papakosta, V. Vega-Garita, Z. Qin, J. Popovic-Gerber, P. Bauer, and M. Zeman, "Estimating battery lifetimes in solar home system design using a practical modelling methodology," *Appl. Energy*, vol. 228, pp. 1629–1639, Oct. 2018, doi: 10.1016/j.apenergy.2018.06.152.

[22] *Classic-Handbook for Stationary Vented Lead-Acid Batteries—Part 2, Installation, Commissioning and Operation*, 4th ed. Büdingen, Germany: Ind. Power, Appl. Eng., GNB a division Exide Technol., Jan. 2012.

[23] A. Millner, "Modeling lithium ion battery degradation in electric vehicles," in *Proc. IEEE Conf. Innov. Technol. for Efficient Reliable Electr. Supply*, Waltham, MA, USA, Sep. 2010, pp. 349–356, doi: 10.1109/CITRES.2010.5619782.

[24] A. Soleimani, V. Vahidinasab, and J. Aghaei, "A linear stochastic formulation for distribution energy management systems considering lifetime extension of battery storage devices," *IEEE Access*, vol. 10, pp. 44564–44576, 2022, doi: 10.1109/ACCESS.2022.3169480.
[25] A. Sorour, M. Fazeli, M. Monfared, A. A. Fahmy, J. R. Searle, and R. P. Lewis, "Forecast-based energy management for domestic PV-battery systems: A U.K. case study," *IEEE Access*, vol. 9, pp. 58953–58965, 2021, doi: 10.1109/ACCESS.2021.3072961.
[26] J. Wang, P. Liu, J. Hicks-Garner, and E. Shermanx, "Cycle-life model for graphite-LiFePO$_4$ cells," *J. Power Sources*, vol. 196, no. 8, pp. 3942–3948, 2011.
[27] W. Chai, Z. Li, X. Cai, and X. Wei, "Variable step-size control method of large capacity battery energy storage system based on the life model," *Trans. China Electrotechn. Soc.*, vol. 14, pp. 58–66, Jul. 2016.
[28] D. Wang, J. Coignard, T. Zeng, C. Zhang, and S. Saxena, "Quantifying electric vehicle battery degradation from driving vs. vehicle-to-grid services," *J. Power Sources*, vol. 332, pp. 193–203, Nov. 2016.
[29] C. Liu, X. Wang, and X. Wu, "A multi-layer dispatch strategy of combined wind-storage systems considering optimization of battery units," *Power Syst. Technol.*, vol. 40, no. 10, pp. 3029–3037, 2016.
[30] S. Drouilhet and B. Johnson, "A battery life prediction method for hybrid power applications," Dept. Energy, Golden, CA, USA, Tech. Rep. NREL/CP-440-21978, 1997.
[31] Y. Yang, W. Pei, W. Deng, Z. Shen, Z. Qi, and M. Zhou, "Day-ahead scheduling optimization for microgrid with battery life model," *Trans. China Electrotech. Soc.*, vol. 30, no. 22, pp. 172–180, Nov. 2015.
[32] M. Shi, J. Hu, H. Han, and X. Yuan, "Design of battery energy storage system based on Ragone curve," in *Proc. 4th Int. Conf. HVDC (HVDC)*, Xi'an, China, 2020, pp. 37–40, doi: 10.1109/HVDC50696.2020.9292767.
[33] M. M. Alhaider, E. M. Ahmed, M. Aly, H. A. Serhan, E. A. Mohamed, and Z. M. Ali, "New temperature-compensated multi-step constant-current charging method for reliable operation of battery energy storage systems," *IEEE Access*, vol. 8, pp. 27961–27972, 2020, doi: 10.1109/ACCESS.2020.2972391.

KRISHNA KUMBA received the B.Tech. degree in electrical and electronics engineering from JNTU Hyderabad, India, in 2008, the M.Tech. degree in the control system from the National Institute of Technology (NIT) Kurukshetra, Haryana, India, in 2010, and the Ph.D. degree from NIT Tiruchirappalli, India, in 2023. He is currently an Assistant Professor with the School of Electrical Engineering, Vellore Institute of Technology, Chennai, Tamil Nadu, India. His research interests include power system planning and reliability, solar photovoltaics, renewable energy systems, solar tracking systems, battery management systems, machine learning, and optimization.

SISHAJ P. SIMON was born in India. He received the B.Eng. degree in electrical and electronics engineering and the M.Eng. degree in applied electronics from Bharathiar University, Coimbatore, Tamil Nadu, India, in 1999 and 2001, respectively, and the Ph.D. degree in power system engineering from Indian Institute of Technology (IIT) Roorkee, Roorkee, Uttarakhand, India, in 2006. Currently, he is an Associate Professor with the Department of Electrical and Electronics Engineering, National Institute of Technology (NIT) Tiruchirappalli (formerly Regional Engineering College), Tiruchirappalli, Tamil Nadu. His research interests include the area of power system operation and control, power system planning and reliability, artificial neural networks, fuzzy logic systems, the application of meta-heuristics, and intelligent techniques to power systems.

VENKATESWARLU GUNDU received the Ph.D. degree from the National Institute of Technology (NIT) Tiruchirappalli (formerly Regional Engineering College), Tamil Nadu, India. He is currently an Assistant Professor with the Department of Computer Science and Engineering, Koneru Lakshamaiah Education Foundation Guntur, Guntur, India. His research interests include the applications of deep learning and soft computing in power systems.

PATRI UPENDER received the B.Tech. degree from JNTU Hyderabad, in 2008, the M.Tech. degree in RF and microwave from Indian Institute of Technology Roorkee, in 2010, and the Ph.D. degree from the National Institute of Technology Warangal, Warangal, in 2023. He is currently an Assistant Professor with the School of Electronics Engineering, Vellore Institute of Technology, Chennai, Tamil Nadu, India. He has about ten years of research experience in the development of antennas and metamaterials. His research interests include biosensing applications, metamaterials, dielectric resonator antennas, microwave, millimeter wave antennas, radar engineering, 5G devices, RF communication, and graphene devices. He has more than 30 publications in various journals and conferences at national and international level.

NAWIN RA received the B.E. degree in electrical and electronics engineering from Anna University, Chennai, India, in 2017, the M.Tech. degree in green energy technology from Pondicherry (Central) University, India, in 2019, and the Ph.D. degree electrical and electronics engineering from the Birla Institute of Technology and Science (BITS)-Pilani, Hyderabad Campus, in 2023. He is currently an Assistant Professor with Vellore Institute of Technology, Chennai Campus. His research interests include energy systems, flow batteries, solar photovoltaics, energy management, power electronic converters, electric vehicles, machine learning, and optimization.

MITHUN SARKAR received the B.Tech. degree in electrical engineering from Kalyani Government Engineering College, India, in 2011, and the M.Tech. degree in power control and drives and the Ph.D. degree from the National Institute of Technology, India, in 2013 and 2019, respectively. He is currently an Assistant Professor with the School of Electrical Engineering, Vellore Institute of Technology, Chennai, India. His research interests include the wide-area control of power systems and robust control and time delay systems.